Video Article

Monitoring the Effects of Illumination on the Structure of Conjugated Polymer Gels Using Neutron Scattering

Brian Morgan[1], Samantha J. Rinehart[1], Mark D. Dadmun[1,2]

[1]Department of Chemistry, University of Tennessee, Knoxville

[2]Chemical Sciences Division, Oak Ridge National Laboratory

Correspondence to: Mark D. Dadmun at dad@utk.edu

URL: https://www.jove.com/video/56163
DOI: doi:10.3791/56163

Keywords: Chemistry, Issue 130, Optically active polymers, conjugated polymers, polymer gels, small angle neutron scattering, stimuli-responsive materials, thermo-reversible

Date Published: 12/21/2017

Citation: Morgan, B., Rinehart, S.J., Dadmun, M.D. Monitoring the Effects of Illumination on the Structure of Conjugated Polymer Gels Using Neutron Scattering. *J. Vis. Exp.* (130), e56163, doi:10.3791/56163 (2017).

Abstract

We demonstrate a protocol to effectively monitor the gelation process of a high concentration solution of conjugated polymer both in the presence and absence of white light exposure. By instituting a controlled temperature ramp, the gelation of these materials can be precisely monitored as they proceed through this structural evolution, which effectively mirrors the conditions experienced during the solution deposition phase of organic electronic device fabrication. Using small angle neutron scattering (SANS) and ultra-small angle neutron scattering (USANS) along with appropriate fitting protocols we quantify the evolution of select structural parameters throughout this process. Thorough analysis indicates that continued light exposure throughout the gelation process significantly alters the structure of the ultimately formed gel. Specifically, the aggregation process of poly(3-hexylthiophene-2,5-diyl) (P3HT) nano-scale aggregates is negatively affected by the presence of illumination, ultimately resulting in the retardation of growth in conjugated polymer microstructures and the formation of smaller scale macro-aggregate clusters.

Video Link

The video component of this article can be found at https://www.jove.com/video/56163/

Introduction

Conjugated polymers promise functional materials that can be utilized in a broad range of devices, such as organic light emitting diodes, organic semiconductors, chemical sensors, and organic photovoltaics.[1,2,3,4,5,6] A crucial aspect of the performance in these devices is the ordering and packing of the conjugated polymer in the solid state in the active layer.[7,8,9,10,11,12,13,14] This morphology is largely pre-determined by both the conformation of the polymer chain in solution as well as the structures that evolve as these solutions are cast unto a substrate and the solvent is removed. By studying the structures present throughout a typical sol-gel transition of a model optoelectronic polymer in a suitable solvent, these systems can be effectively modeled and a quantitative glimpse into the self-assembly that occurs during material deposition can be obtained.[15,16,17,18,19,20]

Specifically, we examine the conjugated polymer benchmark P3HT in the solvent deuterated ortho-dichlorobenzene (ODCB), a polymer-solvent system which has seen extensive use due to its suitability for a variety of organic electronic device fabrication techniques.[23,24,25] In this given solvent environment, P3HT chains begin to aggregate upon an appropriate environmental stimuli, such as temperature decrease or loss of solvent quality. The exact mechanism for this assembly process is under investigation, with one of the leading proposed pathways believed to be a gradual process where individual P3HT molecules π-stack to form lamellar nano-aggregates known as nanofibrils, which then themselves agglomerate to form larger micron scale macro-aggregates.[24] Understanding these pathways and the resultant structures formed is key to properly predicting and influencing the formation of optimal device active layer morphologies.

Towards this ultimate goal of more precisely directing the formation of these active layer architectures, there exists a need to develop additional experimental and industrial methods to non-destructively alter conjugated polymer morphology in-situ. One relatively new methodology centers around the use of light exposure as an inexpensive means for altering polymer chain morphology, with both computational and experimental results pointing towards its feasibility.[25,26,27] Recent work by our laboratory has indicated the existence of a light induced alteration of the conjugated polymer-solvent interaction in a dilute solution, leading to a notable change in polymer chain size upon illumination.[30,31] Here, we present a protocol to continue this work by effectively monitoring the effects of exposing a much more concentrated conjugated polymer solution to direct light throughout a gelation process that is directed by a thermostat-controlled temperature ramp. We employ neutron scattering as it allows robust analysis of structural parameters of the polymer-solvent sol-gel system on length scales from angstroms to microns, an ability not possible through other more common rheological or spectroscopic instrumental methods.[16,17,30,31] Thus, by comparing the properly analyzed small and ultra-small angle neutron data for the assembly of gels formed under illumination to identical data collected in complete darkness, structural differences brought on by illumination-driven effects can be comprehensively identified and quantified.

Protocol

All handling of chemicals should be carried out with proper personal protective equipment and within a safety hood. All samples exposed to ionizing radiation should be handled under the supervision of the facilities radioactive control technicians. This protocol was performed by individuals who had completed appropriate radiation safety training.

1. Preparation of P3HT in d-ODCB Solutions

1. **Sample Acquisition**
    1. Purchase 1 g of high regioregularity (>90%) P3HT in the molecular weight range 15 - 40 K.
    2. Purchase 5 g of high purity (>90 atom% deuterated) d-4 1,2-ODCB.

2. **Sample Preparation**
    1. Filter all d-ODCB solution with 0.45 µm sieve into a glass vial.
    2. Combine 0.34 g of P3HT in 1.66 g of d-ODCB in a 5 g glass vial with foil lined cap.
    NOTE: Throughout the sample creation and transfer process, minimize the ambient light intensity to which the sample is exposed at all times.
    3. Add a magnetic stir bar to the vial, secure the cap, and seal with parafilm.
    4. Wrap vial entirely in aluminum foil to prevent any light exposure to solution.
    5. Place sample on hot plate at 70 °C for 1 - 3 h with the magnetic stir bar enabled.
    6. Remove from heat and stirring once solution is completely homogeneous (preferably leaving the sample heating/stirring overnight to ensure complete dispersion).
    7. Transfer solution from vial to a properly cleaned (with separate rinses of acetone and water) 1 or 2 mm thick quartz banjo cell using a glass pipette.
    NOTE: Heating the glass pipette in a heating oven to 70 °C immediately before transfer greatly simplifies this process.
    8. Affix banjo cell cap and seal with parafilm.
    9. Place banjo cell in complete darkness (i.e. inside a sealed box or wrapped in aluminum foil).
    10. In a similar fashion assemble a sample which contains only d-ODCB (filled to capacity) and an empty banjo cell, to act as the solvent background and empty cell, respectively, for the scattering experiments.

2. Neutron Scattering Experiments

1. **SANS Experiments in the "dark" environment**
    1. With assistance from the instrument scientist, ensure a sample stage is affixed with the required temperature controls capable of directing a temperature ramp from 70 - 20 °C.
    2. Place the banjo cells in the appropriately sized holding blocks, secure, and label.
    3. Wrap entire block with 0.1 mm thick aluminum foil to ensure no ambient light is incident to the sample. Minimize deformations of the foil to ensure proper fitting of the wrapped block in the sample stage. Place this wrapped block and sample within the sample stage.
    4. With assistance from the instrument scientist, complete the proper instrument alignment and calibration using the appropriate standard measurements. Set the detector distance close to its maximum setting (for instance at 18 m) to ensure access to the lowest Q region (~0.001 $Å^{-1}$), ultimately allowing a full Q range of roughly 0.001-0.1 $Å^{-1}$. This will allow probing of length scales up to ~500 nm.
    5. With the assistance of the instrument scientist, collect count rates for the P3HT and solvent samples and perform calculations to determine the amount of scattering time required to achieve total detector counts per sample of roughly 500,000 to 1,000,000, ensuring good statistical quality in the data.
    6. With this information, create a sample script which will direct the 70-20 °C temperature ramp and data collection process. Choose a range of discrete temperature points to best cover the entire range within the given time restraints, for instance every 2 °C. For every point on the ramp make 3 separate entries in the script: a change to the desired temperature, a wait period (~15 minutes) to allow the system to thermally equilibrate before scattering is collected, and the scattering measurement itself conducted over the appropriate time duration to achieve the required detector counts
    7. Once the instrument and script are prepared, execute the script and begin the experiment. Be sure to collect data for the solvent and empty cell as well (without temperature ramp). Additionally, collect transmission data for each sample and a blocked beam measurement.

2. **SANS Experiments in the "light" environment**
    1. Upon completion of the "dark" experiment, move the samples from the stage, place on a secure benchtop, and remove all aluminum foil while observing radiation safety protocols.
    2. Position an optical illuminator featuring a halogen light source near the sample stage such that the leads effectively illuminate the sample slot in the stage associated with the scattering collection position.
    3. Using a calibrated light meter, record the light intensity provided by the illuminator at maximum intensity at the position where the sample will sit. Intensity values will vary with illuminator and sample stage configuration, however, illumination intensity of at least 5,000 lux is desired.
    4. Once this illumination setup is properly assembled, return the samples to the stage, ensure the illuminator is properly lighting the active sample, heat again to 70 °C, allow proper equilibration, and repeat the data collection procedure performed on the dark samples, with the optical illuminator providing uninterrupted direct light exposure thorough the entire duration of this step.

3. **USANS Experiments**

1. Prepare USANS samples in a similar fashion using quartz banjo cells and place in copper or titanium blocks within a temperature controlled sample stage.
2. With the help of the instrument scientist, align and calibrate the instrument employing the requisite number of buffers at the given neutron wavelength to allow analysis of Q values from roughly 10^{-5} - 10^{-3} $Å^{-1}$, allowing length scales on the order of microns to be probed.
3. Develop the experimental script in a similar fashion to the SANS experiments, allowing for thermal equilibration and data collection at each temperature studied previously.
4. Replicate the SANS experiments again, execute the script once under "dark" conditions and again under ""light" conditions.

3. Data Reduction and Analysis

1. **SANS reduction and analysis**
   1. Using the respective reduction program,[32] input the data files for scattering, background (solvent), empty cell, blocked beam, and transmission measurements to accomplish proper background subtraction and conversion of scattering data to absolute units of intensity in cm^{-1}.
   2. With the data appropriately reduced, begin analysis by fitting the experimental scattering data to a model that is the linear addition of two fitting equations, one representing the nanofibril aggregates through the elliptical cylinder model,[33] and another taking into account the free chains in solution through the polymer excluded volume model.[34,35] The equation below describes this combination model approach:
   $$I(q) = \phi_{P3HT}\phi_{ECM}(\Delta\rho_{ECM})^2 P_{ECM}(q) + \phi_{P3HT}(1-\phi_{ECM})(\Delta\rho_{PEV})^2 P_{PEV}(q)$$
   In this equation, ϕ_{P3HT} describes the total volume fraction of P3HT in the solution, ϕ_{ECM} is the volume fraction of aggregated P3HT present and modeled as an elliptical cylinder, P_{PEV} is the free chain excluded volume form factor for P3HT, P_{ECM} describes the elliptical cylinder form factor for the aggregates, and $\Delta\rho_{ECM}$ and $\Delta\rho_{PEV}$ are the scattering length density (SLD) contrast between P3HT aggregates and the solvent and between the free P3HT chains and the solvent, respectively. SLD values for all components of the system can be calculated with a knowledge of their chemical composition and mass density and the use of an SLD calculator available as part of most neutron analysis programs or online.[36]
   3. Upon proper fitting procedures using NCNR Igor fitting macros[37] or the SASView fitting program, acquire values for the key structural parameters for the gelled system at all temperatures in the light and dark, allowing quantification of the morphological evolution occurring throughout this process as a function of temperature and light exposure. These structural parameters include the cross-sectional areas of the nanofibrils, free chain radius of gyration (R_g) and Porod exponent, and a qualitative assessment of the total amount of material present in the nanofibril phase.

2. **USANS reduction and analysis**
   1. Using the respective reduction program, input the scattering data and background data for each buffer to merge the data into a single reduced curve in absolute intensity units of cm^{-1}.
   2. Analyze the data using a Guinier-Porod power law model which allows quantitative assessment of the aggregate scattering patterns probed by the USANS length scale, and allows acquisition of the aggregate R_g values.[38] Fit using this method through NCNR Igor fitting macros[37] or the SASView fitting program to allow comparison of macro-aggregate R_g across all temperatures and illumination conditions.

Representative Results

Through SANS and USANS experiments, the gelation process of P3HT in d-ODCB was effectively monitored from the dispersed solution state at 70 °C to a fully gelled state at 20 °C. These experiments were conducted in both complete darkness and under white light illumination. **Figure 1** displays some example SANS reduced data curves from these experiments, with an example curve fit shown in **Figure 2**. From this data, the structural changes occurring as temperature decreases have been effectively captured, denoted by a clear increase in absolute intensity as temperature falls. Additionally, for each given temperature there is a clear discrepancy between the scattering data of the samples studied in the dark and those studied in the light as the data plots do not overlap. This indicates that light exposure significantly affects the aggregation process. **Figure 3** displays values for a variety of structural parameters extracted using the combined fit model from the SANS data and provides structural information on both the nanofibril aggregates and the free chains still in solution. The nanofibril surface area describes the surface area of the face of the cylindrical nano-scale P3HT aggregates and the ECM scale factor gives a qualitative description of the amount of P3HT present in the aggregate phase, while the free chain R_g and Porod exponent describe the size and form factor of the P3HT chains not yet gelled in the solution. Significant differences in these parameters at each given temperature and between light and dark samples at a given temperature indicate that the experiment and fitting process have captured the effect of light exposure on this gelation process. Since they employ a substantially lower Q range, USANS experiments allow the characterization of larger length scales consistent with P3HT macro aggregates, and by mirroring the same approach used in the SANS experiments, the effect of temperature and light upon the size of these aggregates is effectively quantified. **Figure 4** shows USANS data plotted alongside the SANS data for a single temperature, and **Figure 5** displays the R_g data acquired through fitting USANS data with a power law model. This R_g value grows with decreasing temperature as gelation progresses and individual P3HT nanofibrils themselves aggregate to form large scale microstructures. And as with the SANS data, there exists clear difference between the light and dark data, specifically showing smaller R_g values with light exposure.

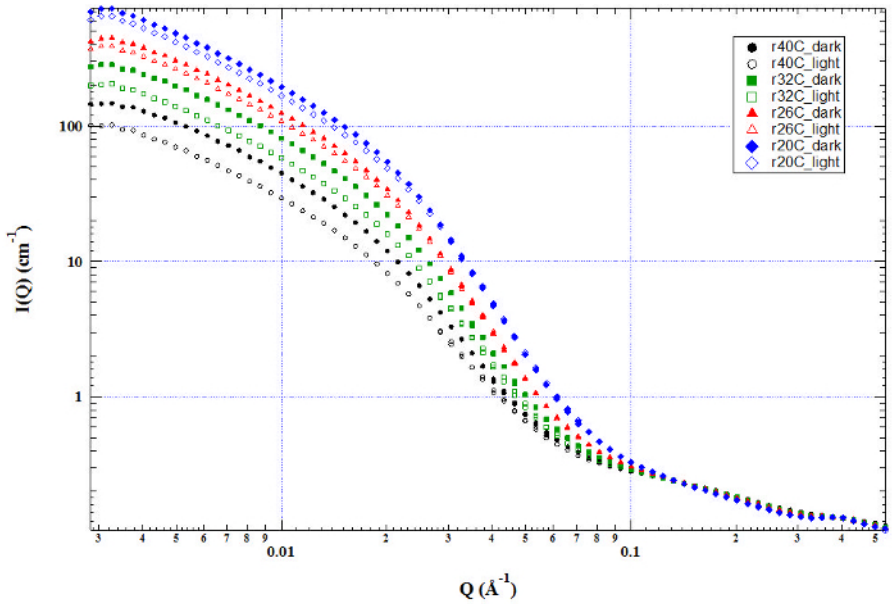

Figure 1: Small angle neutron scattering data for a 17 wt% sample of P3HT in d-ODCB through 70-20 °C temperature ramp. Data collected under white light illumination (open symbols) and in complete darkness (closed symbols). Error bars report instrumental error. Reproduced from reference 28 with permission. Please click here to view a larger version of this figure.

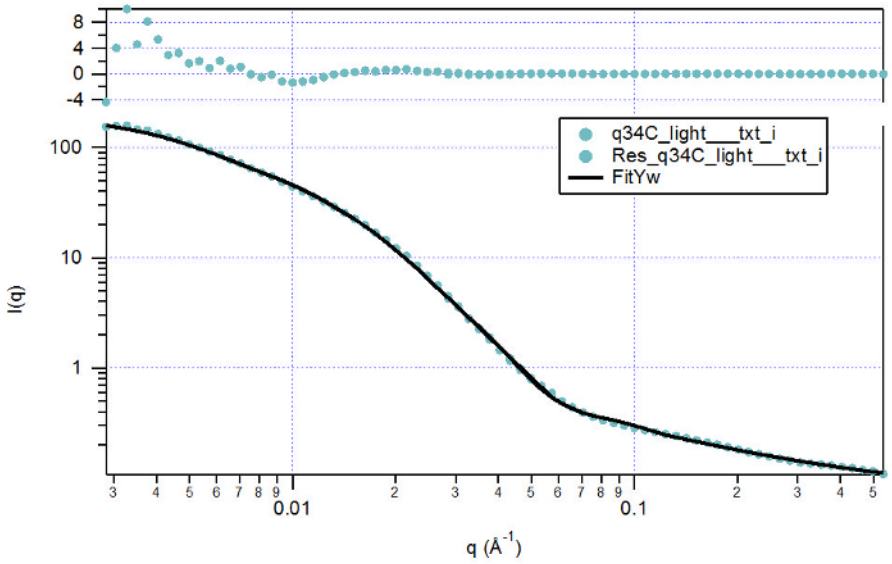

Figure 2: Example fit using a combination model approach incorporating both the Elliptical Cylinder and Polymer Excluded Volume Model to 17 wt% P3HT SANS data collected at 34 °C in the presence of white light illumination. Reproduced from reference 28 with permission. Please click here to view a larger version of this figure.

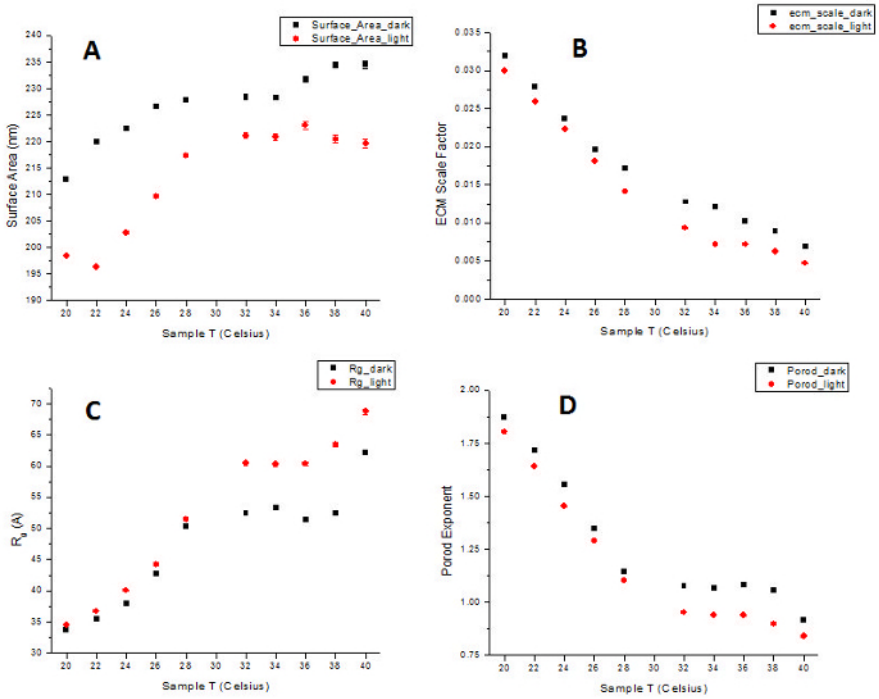

Figure 3: Select parameters obtained from the combined model fit for 17 wt% P3HT through a 70 - 20°C temperature ramp, with black traces indicating samples studied in the dark, and red traces indicating samples studied under illumination: (**A**): nanofibril surface area, (**B**): Elliptical Cylinder Model scale factor, (**C**): radius of gyration of free chains, and (**D**): Porod exponent of free chains. Error bars report fit-generated standard deviation error values. Reproduced from reference 28 with permission. Please click here to view a larger version of this figure.

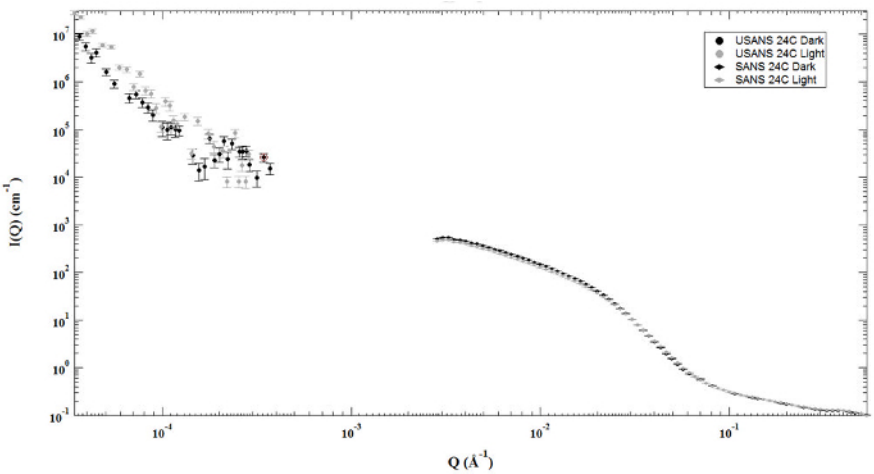

Figure 4: Small and ultra-small angle scattering data of 17 wt% P3HT at 24°C for both illuminated (gray) and dark (black) samples. Error bars report instrumental error. Reproduced from reference 28 with permission. Please click here to view a larger version of this figure.

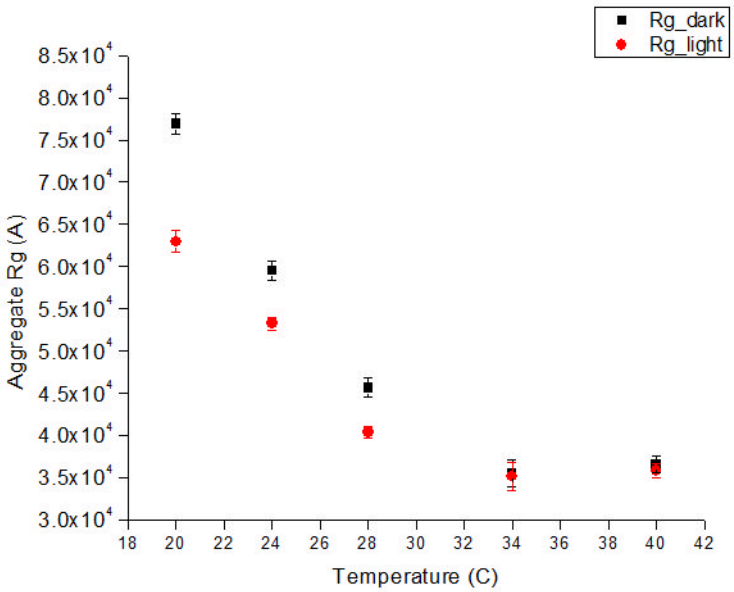

Figure 5: Radius of gyration values obtained from 17 wt% P3HT USANS data fit with a Guinier-Porod power law model for both illuminated (red) and dark (black) samples. Error bars report fit-generated standard deviation error values. Reproduced from reference 28 with permission.

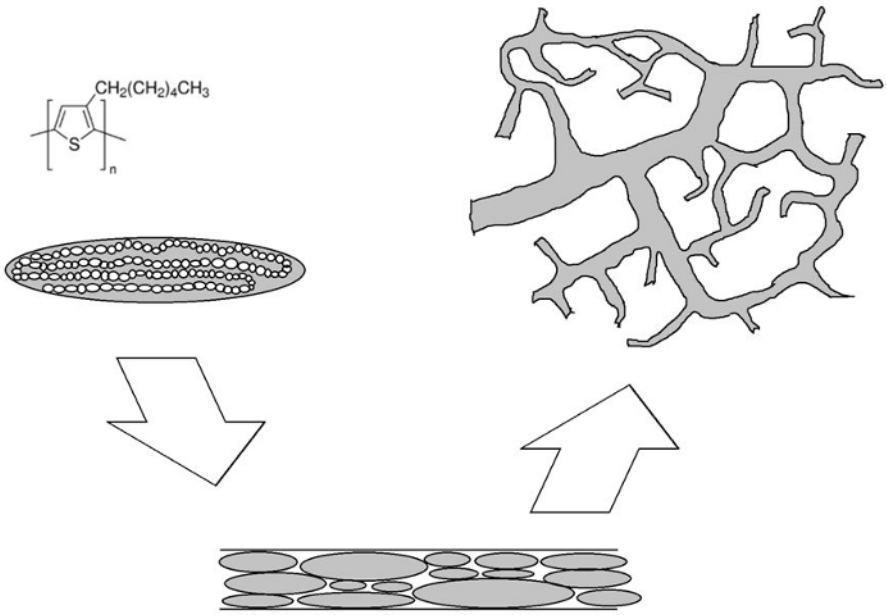

Figure 6: Illustration of the P3HT assembly process from free chains to final micron-scale aggregates. Reproduced from reference 28 with permission. Please click here to view a larger version of this figure.

Discussion

First, looking at the SANS data as a function of temperature, the increase in the Elliptical Cylinder Model scale factor indicates a marked increase in the amount of P3HT present in the nanofibril phase, which isconsistent with the progression of the gelation process. Simultaneously, the decrease in free chain R_g paired with an increase in Porod exponent reveals that the deteriorating thermodynamic conditions associated with temperature decrease are causing a chain collapse in the P3HT chains still present in solution. These results, combined with the USANS data showing a marked increase in macroaggregate R_g upon temperature decrease, indicate that the scattering experiments have effectively captured and analyzed the progression of the structural self-assembly process central to the sol-gel transition, a process that is visualized in **Figure 6**. Analyzing the results of these experiments as a function of light exposure provides further information related to the effect of illumination on the gelation process and the ultimate aggregate structures formed. Comparison of all SANS parameters in **Figure 2** reveals differences between the light and dark samples over a range of temperatures, as does the USANS data in **Figure 3**. Taken together, this information indicates that light exposure effectively hinders the P3HT aggregation process, resulting in less material aggregating in the nanofibril phase (indicated by the ECM scale factor results) and smaller micron scale aggregates (given by the USANS R_g values). Thus, this experiment has also emphasized the

differences between conjugated polymer gelation conducted in the light versus the dark and underlined the importance of illumination conditions upon the device-relevant active layer morphologies which are formed.

When considering a similar experimental approach to the above method it is important to keep in mind the limitations inherent to the system. Neutron scattering is a powerful technique for analyzing angstrom to nanometer scale structures in polymer systems, however, length scales that lie above or below this range are better probed by other techniques. Additionally, if one of the components of the polymer system of interest are not easily deuterated, it can be difficult to achieve the level of contrast necessary for acceptable results. Also, given the limited amount of neutron beam time, experiments must be carefully planned with a relatively concentrated focus. It is also important to have an appropriate robust fitting model pre-determined before the experiments begin to narrow the scope of the analysis process and ensure proper modeling of the system.

Assuming that an experiment meets these conditions, these neutron scattering methods offer a unique tool to unobtrusively monitor the structural evolution of polymer systems over a range of length scales as a function of multiple environmental stimuli, such as temperature and light exposure. Harnessing these approaches could allow for the expansion of these methods to a huge variety of polymer-solvent systems to explore structural changes occurring due to changes in a variety of conditions including (but not limited to) polymer concentration, solvent quality, dopant addition, and thermal history.

Disclosures

The authors have nothing to disclose.

Acknowledgements

The authors gratefully acknowledge the National Science Foundation (DMR-1409034) for support of this project. We also acknowledge the support of the National Institute of Standards and Technology, U.S. Department of Commerce, in providing the USANS facilities used in this work, where these facilities are supported in part by the National Science Foundation under Agreement No. DMR-0944772. The SANS experiments of this research were completed at ORNL's High Flux Isotope Reactor, which was sponsored by the Scientific User Facilities Division, Office of Basic Energy Sciences, US Department of Energy.

References

1. Günes, S., Neugebauer, H., Sariciftci, N. S. Conjugated Polymer-Based Organic Solar Cells. *Chem. Rev.* **107** (4), 1324-1338 (2007).
2. Burroughes, J. H., *et al.* Light-Emitting Diodes Based on Conjugated Polymers. *Letters to Nature.* **1990**, 539-541 (1990).
3. Coakley, K. M., McGehee, M. D. Conjugated Polymer Photovoltaic Cells. *Chem. Mater.* **16** (23), 4533-4542 (2004).
4. Tyler McQuade, D., Pullen, A. E., Swager, T. M. Conjugated Polymer-Based Chemical Sensors. *Chem. Rev.* **100** (7), 2537-2574 (2000).
5. Wang, X., *et al.* Self-Stratified Semiconductor/dielectric Polymer Blends: Vertical Phase Separation for Facile Fabrication of Organic Transistors. *J. Mater. Chem. C.* **1** (25), 3989 (2013).
6. Segalman, R., McCulloch, B., Kirmayer, S., Urban, J. Block Copolymers for Organic Optoelectronics. *Macromolecules.* **42** (23), 9205-9216 (2009).
7. Chen, H., Hsiao, Y., Hu, B., Dadmun, M. Control of Morphology and Function of Low Band Gap Polymer-bis-Fullerene Mixed Heterojunctions in Organic Photovoltaics with Selective Solvent Vapor Annealing. *J. Mater. Chem. A.* **2**, 9883 (2014).
8. Li, Y., Vamvounis, G., Holdcroft, S. Tuning Optical Properties and Enhancing Solid-State Emission of Poly (Thiophene) S by Molecular Control ,: A Postfunctionalization Approach. *Macromolecules.* **35**, 6900-6906 (2002).
9. Nguyen, T.-Q., Martini, I. B., Liu, J., Schwartz, B. J. Controlling Interchain Interactions in Conjugated Polymers: The Effects of Chain Morphology on Exciton−,Exciton Annihilation and Aggregation in MEH−,PPV Films. *J. Phys. Chem. B.* **104** (2), 237-255 (2000).
10. Chen, H., Hu, S., Zang, H., Hu, B., Dadmun, M. Precise Structural Development and Its Correlation to Function in Conjugated Polymer: Fullerene Thin Films by Controlled Solvent Annealing. *Adv. Funct. Mater.* **23**, 1701-1710 (2013).
11. Schwartz, B. J. Conjugated Polymers as Molecular Materials: How Chain Conformation and Film Morphology Influence Energy Transfer and Interchain Interactions. *Annu. Rev. Phys. Chem.* **54** (3), 141-172 (2003).
12. Haugeneder, A., *et al.* Exciton Diffusion and Dissociation in Conjugated Polymer/fullerene Blends and Heterostructures. *Phys. Rev. B.* **59** (23), 15346-15351 (1999).
13. Sirringhaus, H., *et al.* Two-Dimensional Charge Transport in Self-Organized, High-Mobility Conjugated Polymers. *Nature.* **401** (6754), 685-688 (1999).
14. Al-Ibrahim, M., Ambacher, O., Sensfuss, S., Gobsch, G. Effects of Solvent and Annealing on the Improved Performance of Solar Cells Based on poly(3-Hexylthiophene): Fullerene. *Appl. Phys. Lett.* **86**, 201120 (2005).
15. Koppe, M., *et al.* Influence of Molecular Weight Distribution on the Gelation of P3HT and Its Impact on the Photovoltaic Performance. *Macromolecules.* **42**, 4661-4666 (2009).
16. Malik, S., Jana, T., Nandi, A. K. Thermoreversible Gelation of Regioregular poly(3-Hexylthiophene) in Xylene. *Macromolecules.* **34** (2), 275-282 (2001).
17. Xu, W., *et al.* Sol-gel Transition of poly(3-Hexylthiophene) Revealed by Capillary Measurements: Phase Behaviors, Gelation Kinetics and the Formation Mechanism. *Soft Matter.* **8**, 726 (2012).
18. Chan, K. H. K., Yamao, T., Kotaki, M., Hotta, S. Unique Structural Features and Electrical Properties of Electrospun Conjugated Polymer poly(3-Hexylthiophene) (P3HT) Fibers. *Synth. Met.* **160** (23-24), 2587-2595 (2010).
19. Wicklein, A., Ghosh, S., Sommer, M., Würthner, F., Thelakkat, M. Self-Assembly of Semiconductor Organogelator Nanowires for Photoinduced Charge Separation. *ACS Nano.* **3** (5), 1107-1114 (2009).
20. Newbloom, G. M., Weigandt, K. M., Pozzo, D. C. Electrical, Mechanical, and Structural Characterization of Self-Assembly in poly(3-Hexylthiophene) Organogel Networks. *Macromolecules.* **45**, 3452-3462 (2012).

21. Li, L., Tang, H., Wu, H., Lu, G., Yang, X. Effects of Fullerene Solubility on the Crystallization of poly(3-Hexylthiophene) and Performance of Photovoltaic Devices. *Org. Electron. physics, Mater. Appl.* **10** (7), 1334-1344 (2009).
22. Bu, L., Pentzer, E., Bokel, F. A., Emrick, T., Hayward, R. C. Growth of Polythiophene / Perylene Tetracarboxydiimide Donor / Acceptor Shish-Kebab Nanostructures by Coupled Crystal Modi Fi Cation. *ACS Nano.* **6** (12), 10924-10929 (2012).
23. Yang, X., *et al.* Nanoscale Morphology of High-Performance Polymer Solar Cells. *Nano Lett.* **5** (4), 579-583 (2005).
24. Newbloom, G. M., Kim, F. S., Jenekhe, S. a., Pozzo, D. C. Mesoscale Morphology and Charge Transport in Colloidal Networks of Poly(3-Hexylthiophene). *Macromolecules.* **44**, 3801-3809 (2011).
25. Tretiak, S., Saxena, A., Martin, R., Bishop, A. Conformational Dynamics of Photoexcited Conjugated Molecules. *Phys. Rev. Lett.* **89** (9), 97402 (2002).
26. Botiz, I., Freyberg, P., Stingelin, N., Yang, A. C.-M., Reiter, G. Reversibly Slowing Dewetting of Conjugated Polymers by Light. *Macromolecules.* **46,** 2352-2356 (2013).
27. Botiz, I., *et al.* Enhancing the Photoluminescence Emission of Conjugated MEH-PPV by Light Processing. *ACS Appl. Mater. Interfaces.* **6** (7), 4974-4979 (2014).
28. Morgan, B., Dadmun, M. D. Illumination Alters the Structure of Gels Formed from the Optoelectronic Material P3HT. *Polymer.* **108**, 313-321 (2017).
29. Morgan, B., Dadmun, M. D. Illumination of Conjugated Polymer in Solution Alters Its Conformation and Thermodynamics. *Macromolecules.* **49** (9), 3490-3496 (2016).
30. Ilavsk, M. Phase Transition in Swollen Gels. 2. Effect of Charge Concentration on the Collapse and Mechanical Behavior of Polyacrylamide Networks. *Macromolecules.* **15**, 782-788 (1982).
31. Tanaka, T. Collapse of Gels and the Critical Endpoint. *Phys. Rev. Lett.* **40** (12), 820-823 (1978).
32. NIST. *SANS & USANS Data Reduction and Analysis.* https://www.ncnr.nist.gov/programs/sans/data/red_anal.html (2017).
33. Feigin, L., Svergun, D. *Structure Analysis by Small-Angle X-Ray and Neutron Scattering.* Plenum: New York, (1987).
34. Mittelbach, P. Zur Rontgenkleinwinkelstreuung verdunnter kolloider systeme. *Acta Phys. Austriaca.* **14**, 185-211 (1961).
35. Schulz, G. *Z.* Über die Kinetik der Kettenpolymerisationen. *Phys. Chem.* **43**, 25 (1935).
36. NIST. *Neutron activation and scattering calculator.* https://www.ncnr.nist.gov/resources/activation (2017).
37. Kline, S. R. Reduction and Analysis of SANS and USANS Data Using IGOR Pro. *J. Appl. Crystallogr.* **39** (6), 895-900 (2006).
38. Guinier, A., Fournet, G. *Small-Angle Scattering of X-Rays.*, John Wiley and Sons: New York, (1955).

